

Supporting Information for

**NiS₂ nanoparticles anchored on open carbon nanohelmets as advanced anode for
lithium-ion batteries**

D. D. Yang, M. Zhao, R. D. Zhang, Y. Zhang, C. C. Yang*, and Q. Jiang

Key Laboratory of Automobile Materials (Jilin University), Ministry of Education, and School of Materials Science and Engineering, Jilin University, Changchun 130022, China.

** Corresponding author. Tel.: +86-431-85095371; Fax: +86-431-85095876; E-mail: ccyang@jlu.edu.cn (C. C. Yang).*

† Electronic Supplementary Information (ESI) available. See DOI: 10.1039/x0xx00000x.

Experimental section

Materials synthesis: The synthesis process of NiO nanoparticles/carbon nanohelmets (NiO/CNHs) is referred to our previous work [Ref.²⁸ of the text]. First, the as-prepared NiO/CNHs was dried in a vacuum oven at 70 °C for 12 h. Then, 0.2 g black NiO/CNHs powder and 0.9 g sublimed sulfur were mixed in an agate mortar and entirely ground for 10 min. In a nitrogen atmosphere, the mixture was placed at a small quartz boat and heated at 300 °C for 2 h with a ramp rate of 5 °C min⁻¹. After that, the temperature was heated to 500 °C with a ramp rate of 2 °C min⁻¹ and kept for another 2 h. The furnace was subsequently cooled down to ambient temperature with continuous flowing nitrogen to obtain NiS₂/CNHs. For a comparison, the pristine NiS₂ was also fabricated by the similar process except for adding resorcinol and formaldehyde resin/SiO₂ spheres (RF/SiO₂).

Materials characterization: X-ray diffraction (XRD) measurements were carried out on a D/max2500pc diffractometer with Cu-K α radiation. The microstructure and morphology of the samples were observed with transmission electron microscopy (TEM, JEM-2100F, JEOL, 200 keV) and field-emission scanning electron microscope (FESEM, JSM-6700F, JEOL, 15 keV). Raman spectrum was recorded on a micro-Raman spectrometer (Renishaw) using a 532-nm laser as an excitation source. X-ray photoelectron spectroscopy (XPS) analysis was performed on a Thermo ESCALAB-250Xi spectrometer. The specific area and pore size distribution were determined by nitrogen adsorption and desorption using a Micromeritics ASAP 2020 analyzer. The constituent of the specimen was tested by thermogravimetric analysis (TGA) in air flow from 30 to 1000 °C with a heating rate of 10 °C min⁻¹ using an SDT Q600 instrument.

Electrochemical Measurements: The electrochemical measurements for lithium-ion batteries (LIBs) were performed on coin-type half cells (CR2025) with a metallic lithium foil as both the counter and reference electrode, Celgard (2500) membrane as the separator and 1.0 M LiPF₆ dissolved in the mixture of ethylene carbonate and dimethyl carbonate (EC/DMC, volume ratio of 1:1) as the electrolyte, which were assembled in an argon-filled glove box ([O₂] < 1 ppm and [H₂O] < 1 ppm). The working electrodes were manufactured by mixing active material (NiS₂/CNHs), conductive material (Super P) and binder (polyvinylidene fluoride, PVDF) with the weight ratio of 7:2:1 using N-methyl-2-pyrrolidone (NMP) as a solvent, which were pasted on Cu foil and dried in vacuum at 100 °C for 12 h. Then the electrodes were cut into wafers with a diameter of 12 mm and weighed. The mass loading of active materials for each electrode is 0.55-0.75 mg. The galvanostatic charge/discharge cycling tests were carried out using a LAND CT2001A battery testing system in a voltage range of 0.01-3.0 V. Cyclic voltammetry (CV) tests were implemented on an IVIUM electrochemical workstation (Ivium Technologies) with a potential scan rate of 0.1 mV s⁻¹ within the potential range between 0.01-3.0 V (vs. Li⁺/Li). The electrochemical impedance spectroscopy (EIS) measurements were conducted by applying an amplitude of 10 mV over the frequency range of 100 kHz to 10 mHz at room temperature. In order to evaluate the structural stability of NiS₂/CNHs electrode material, after electrochemical tests for 2000 cycles, the electrodes were disassembled from the cells in an argon-filled glove box ([O₂] < 1 ppm and [H₂O] < 1 ppm) and then rinsed with dimethyl carbonate and ethanol to remove the residual electrolyte. After that, the electrode material and the copper foil were separated by ultrasonic dispersion to obtain a homogeneous mixture, and the subsequent TEM and FESEM characterization were performed.

Supplementary Figures

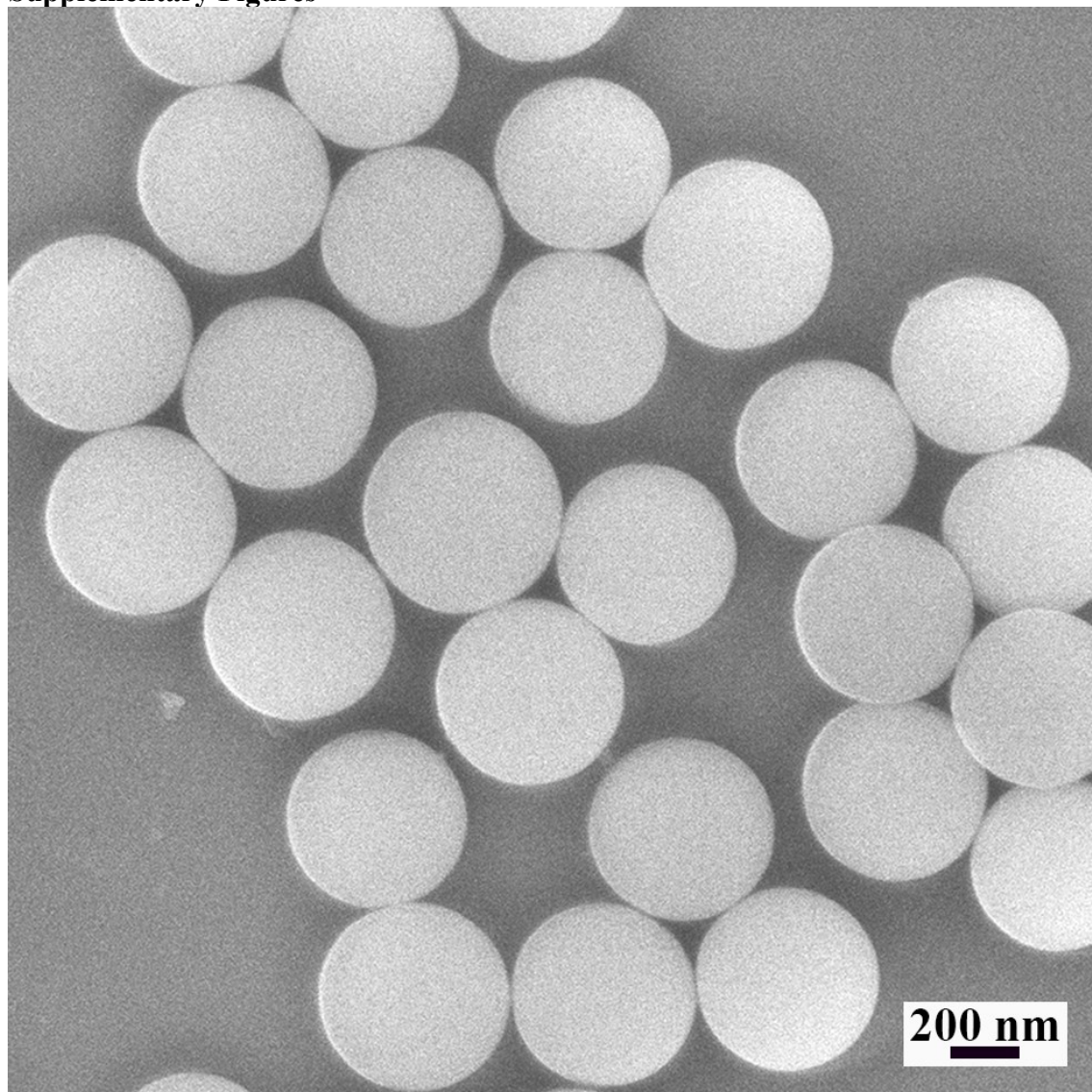


Fig. S1. FESEM image of SiO₂ spheres.

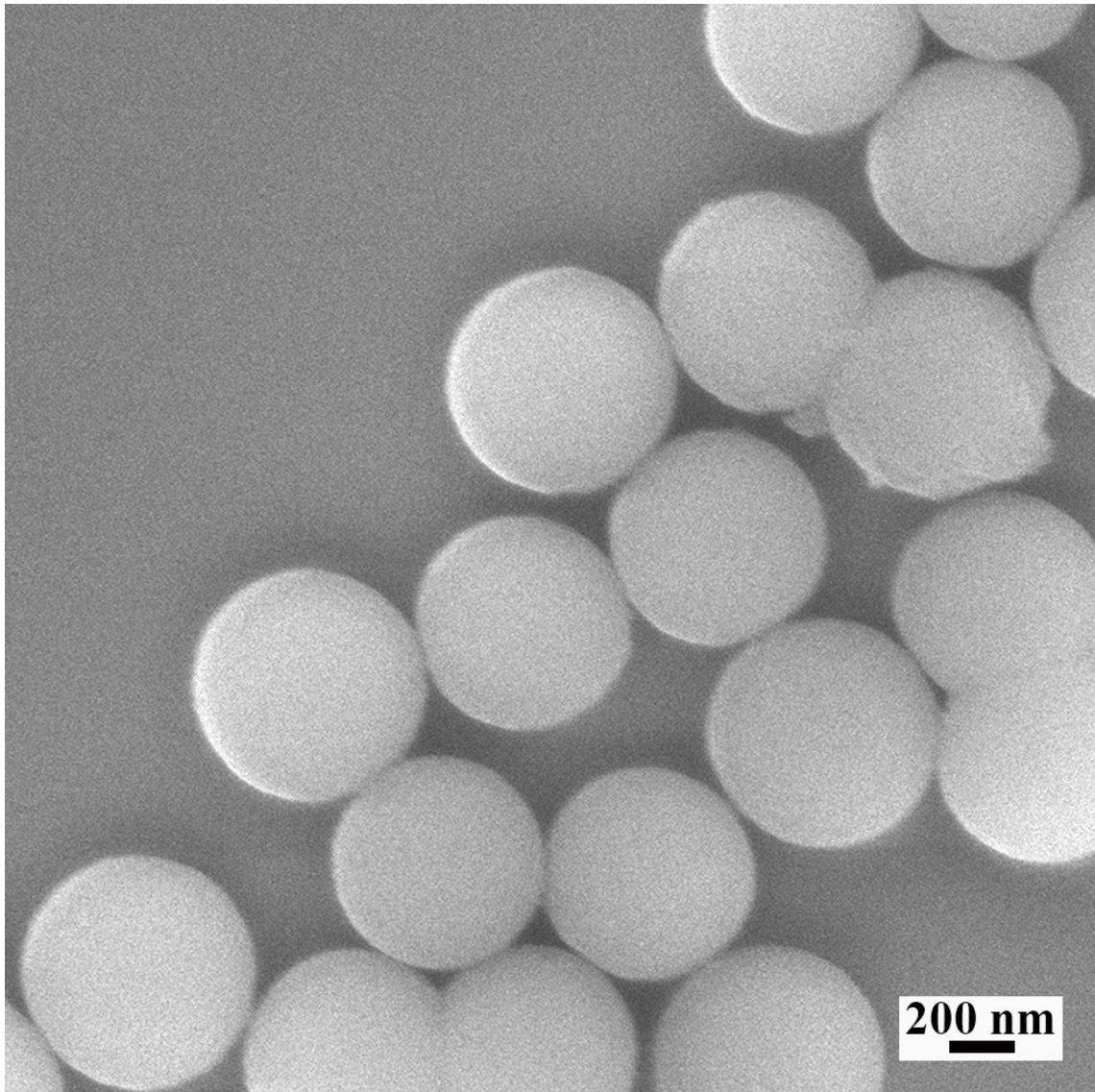


Fig. S2. FESEM image of RF/SiO₂.

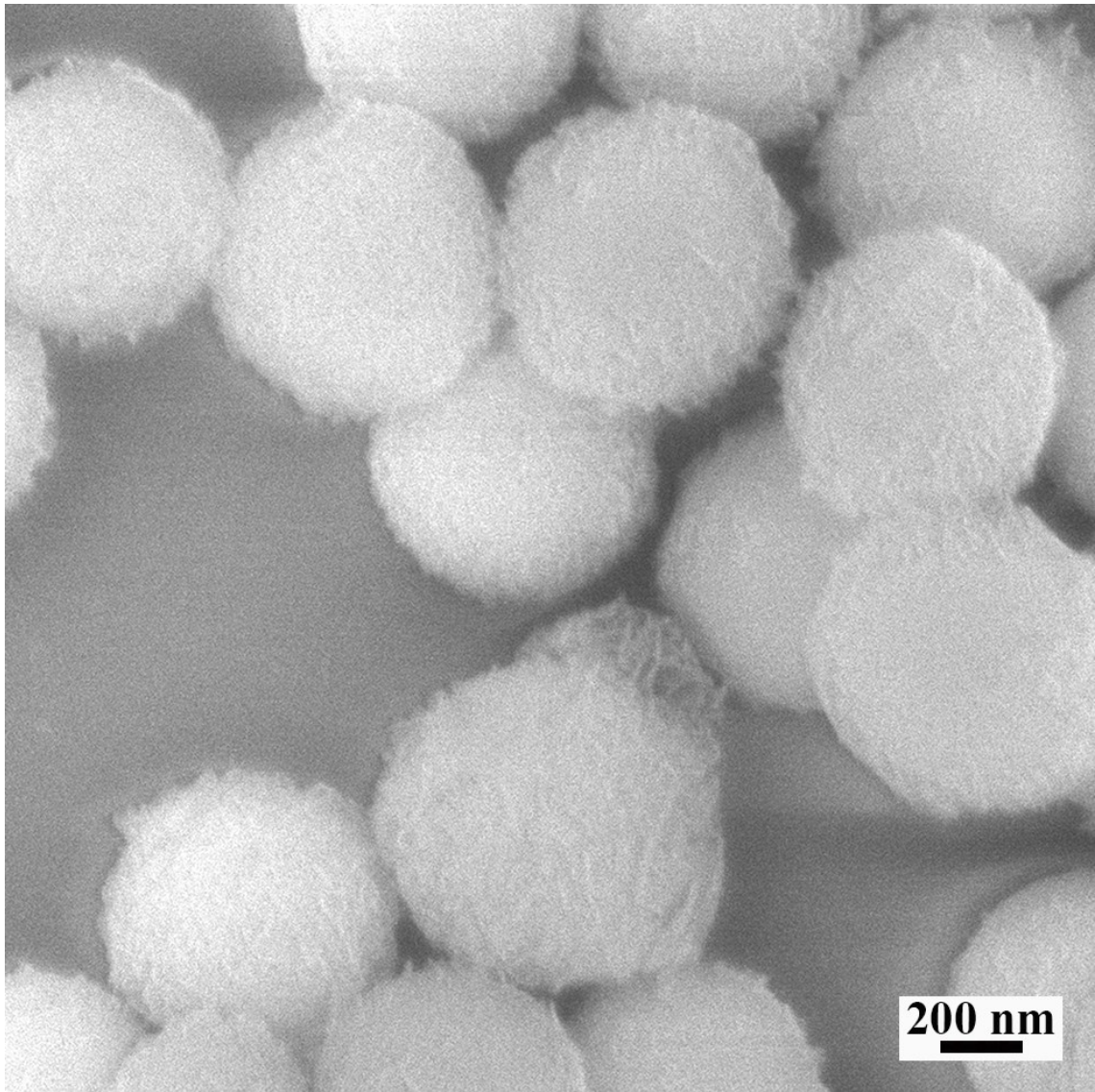


Fig. S3. FESEM image of Ni(OH)₂/RF/SiO₂.

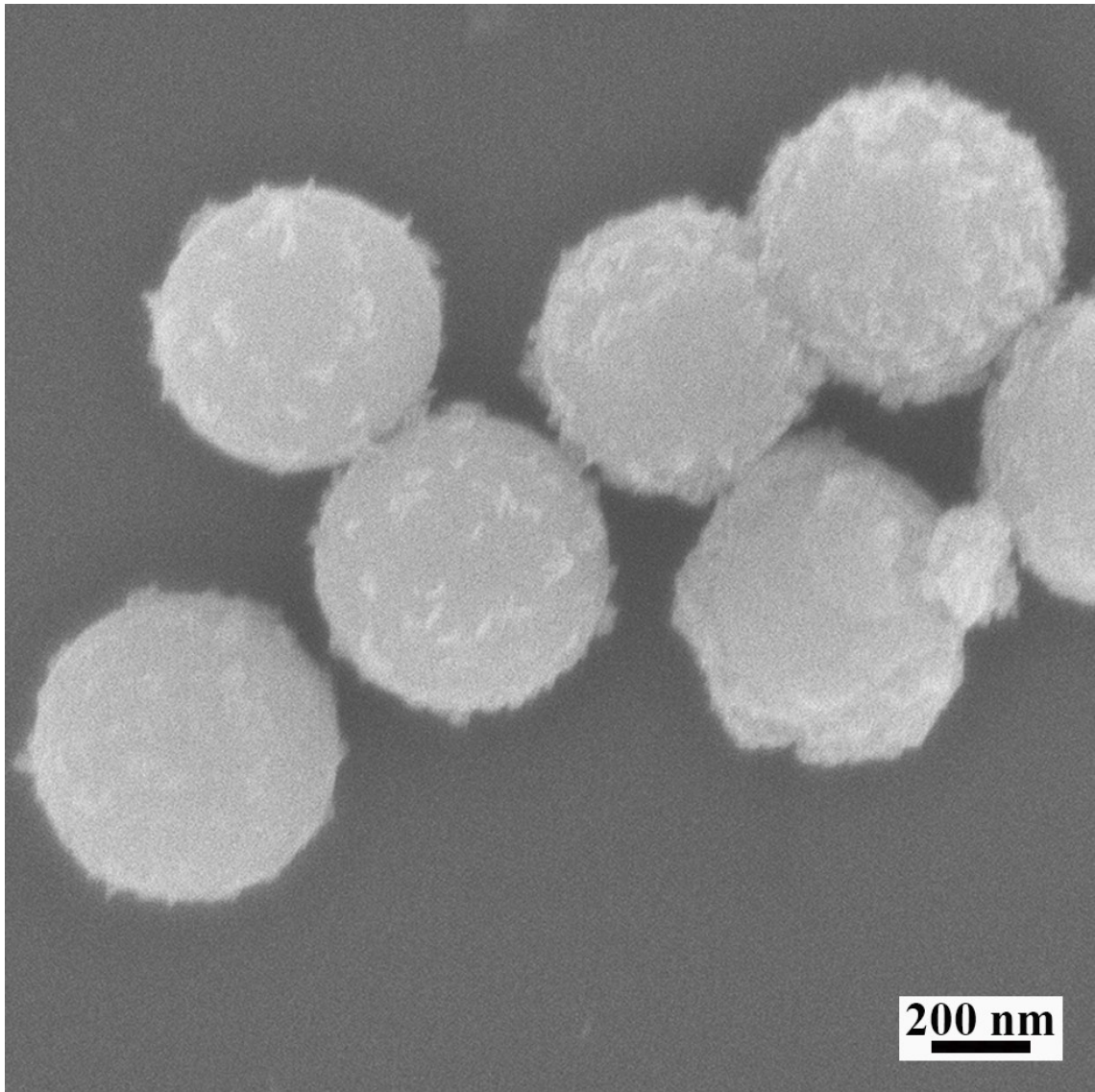


Fig. S4. FESEM image of NiO/C/SiO₂.

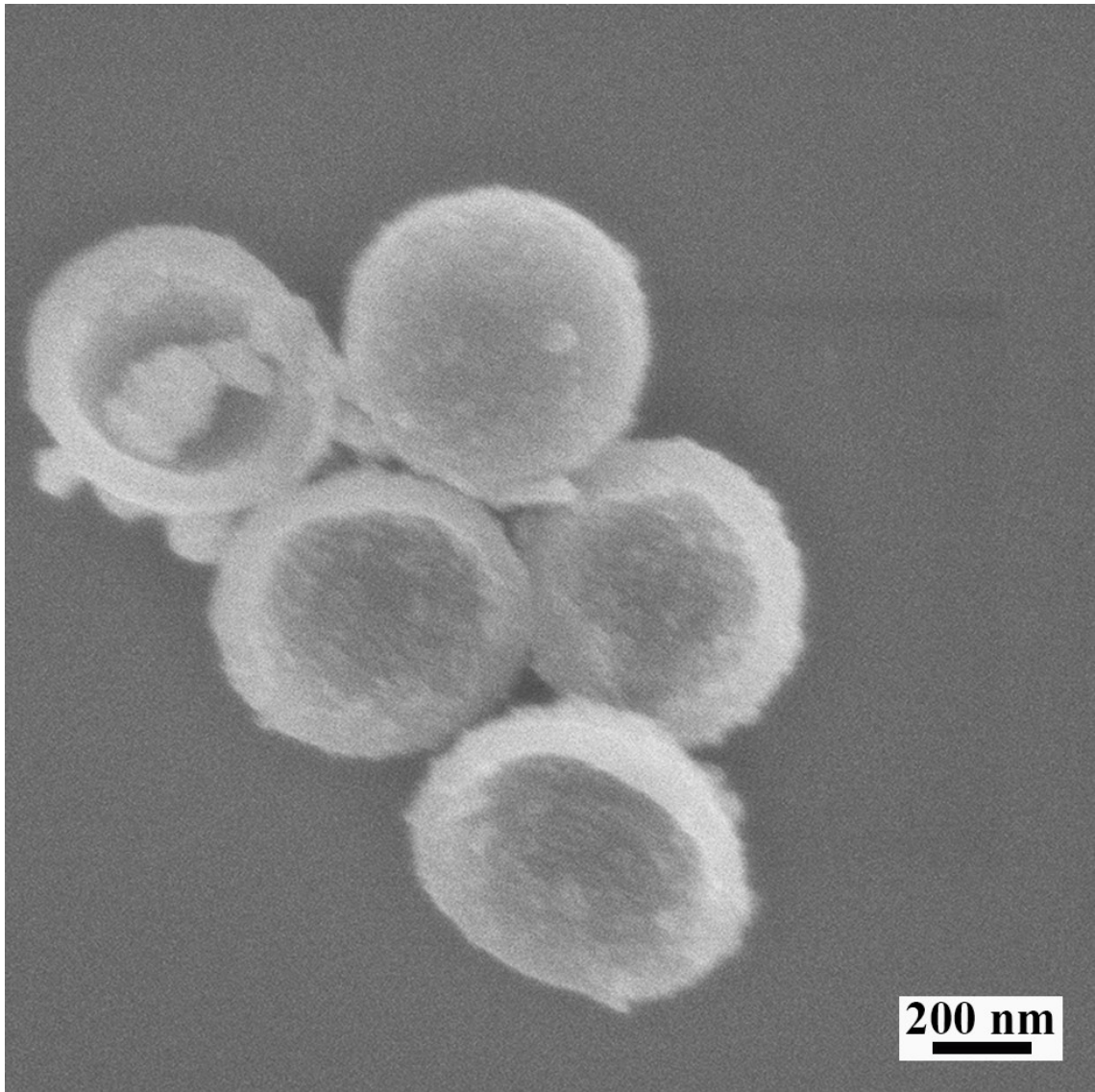


Fig. S5. FESEM image of NiO/CNHs.

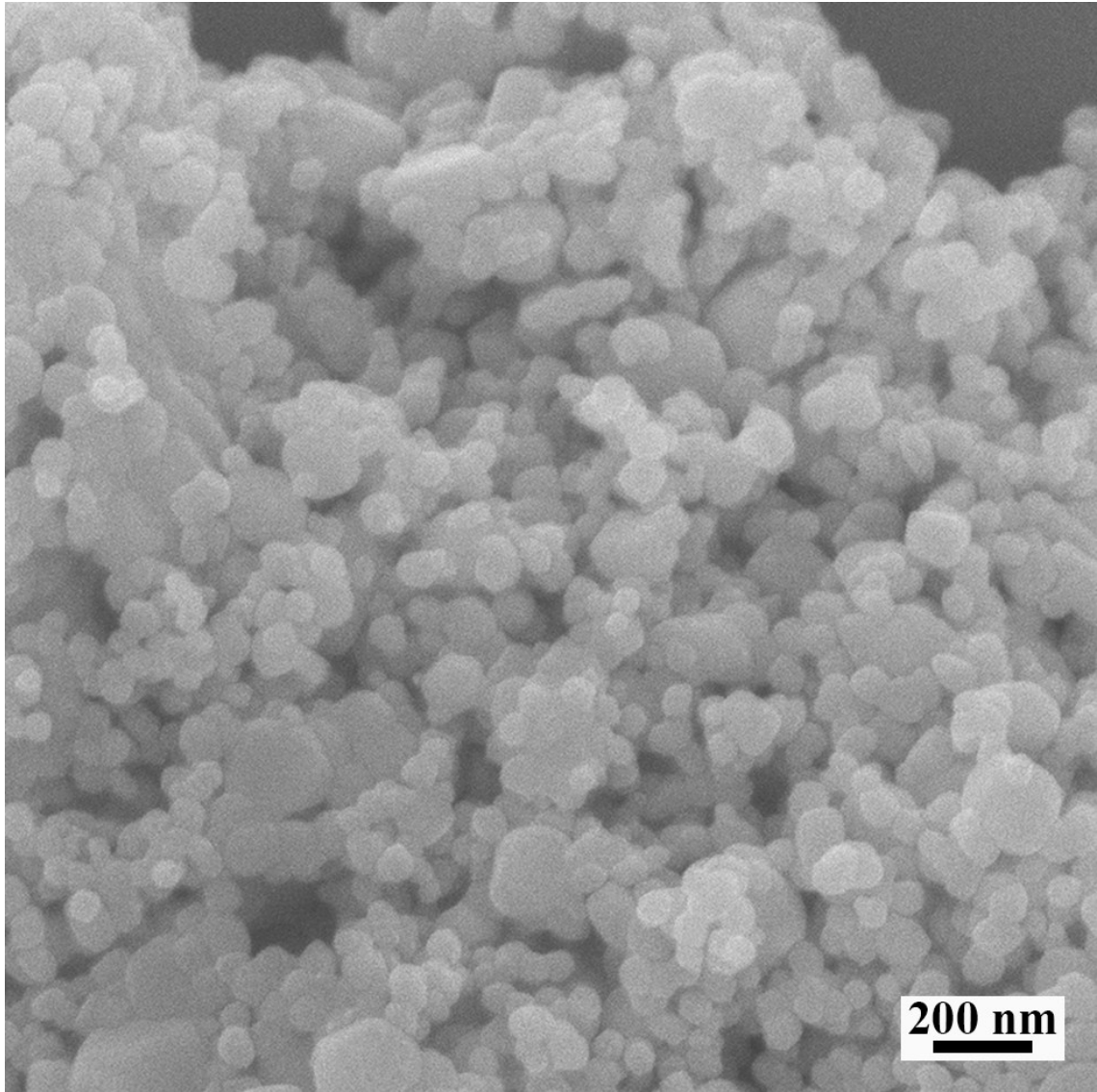


Fig. S6. FESEM image of pristine NiS₂.

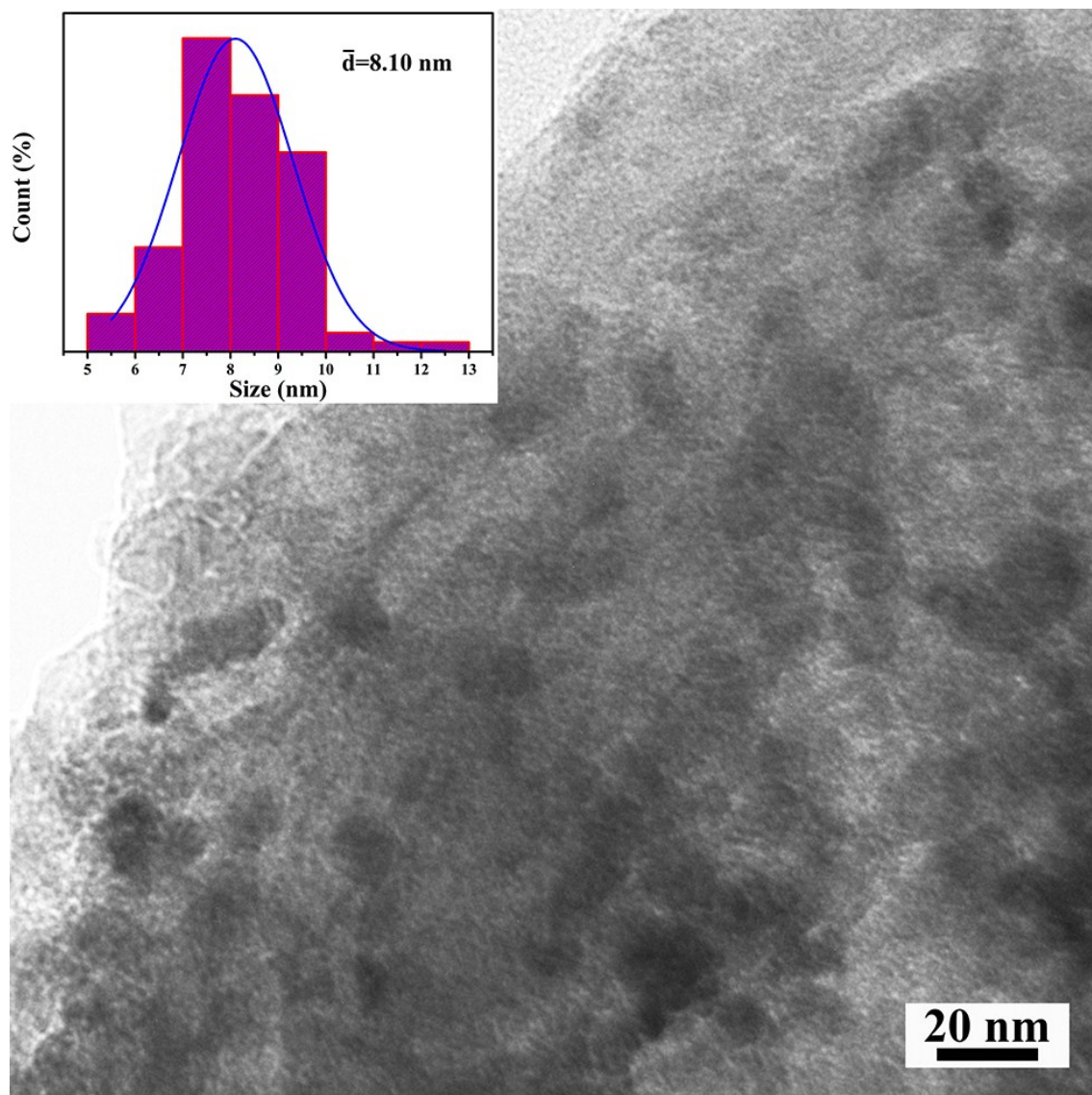


Fig. S7. TEM image and particle size distribution (the inset) of NiS₂/CNHs.

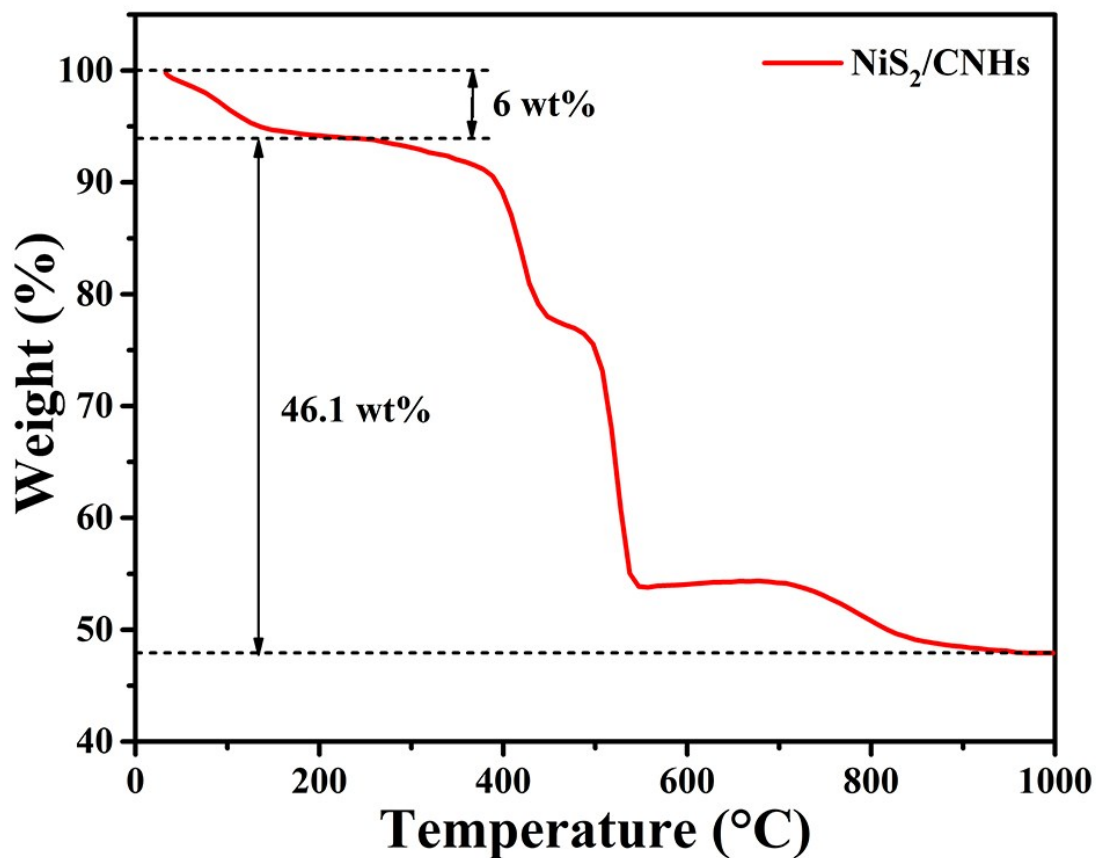


Fig. S8. TGA curve of NiS₂/CNHs.

$$\text{NiS}_2(\text{wt}\%) = \frac{\text{molecular weight of NiS}_2}{\text{molecular weight of NiO}} \times \frac{\text{weight of NiO}}{\text{weight of NiS}_2/\text{CNHs}} \times 100\% = \frac{122.8}{74.7} \times \frac{1 - 0.060 - 0.461}{1 - 0.060} \times 100\% = 83.8\%$$

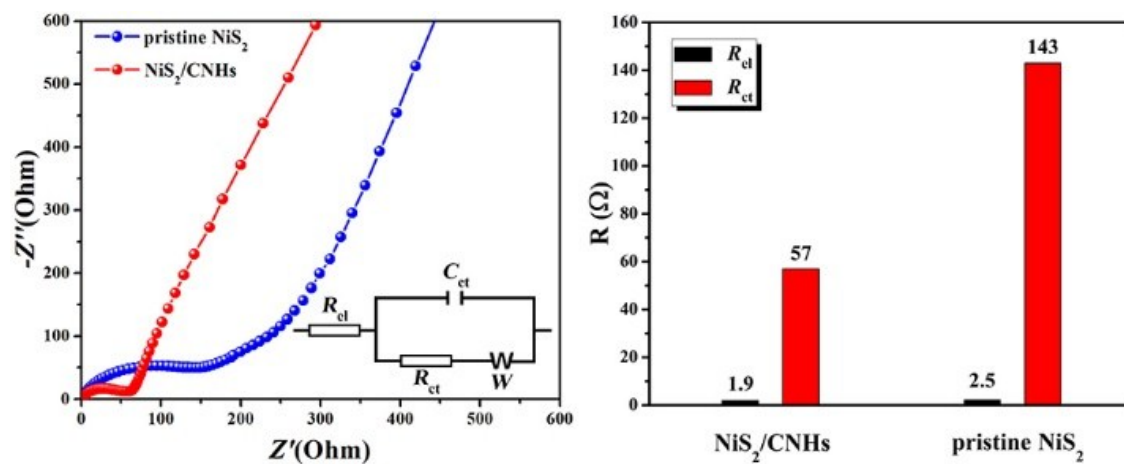


Fig. S9. (a) EIS of pristine NiS₂ and NiS₂/CNHs electrodes in fresh LIBs, where the inset shows the equivalent circuit diagram. (b) Comparisons of R_{cl} and R_{ct} values of pristine NiS₂ and NiS₂/CNHs electrodes.

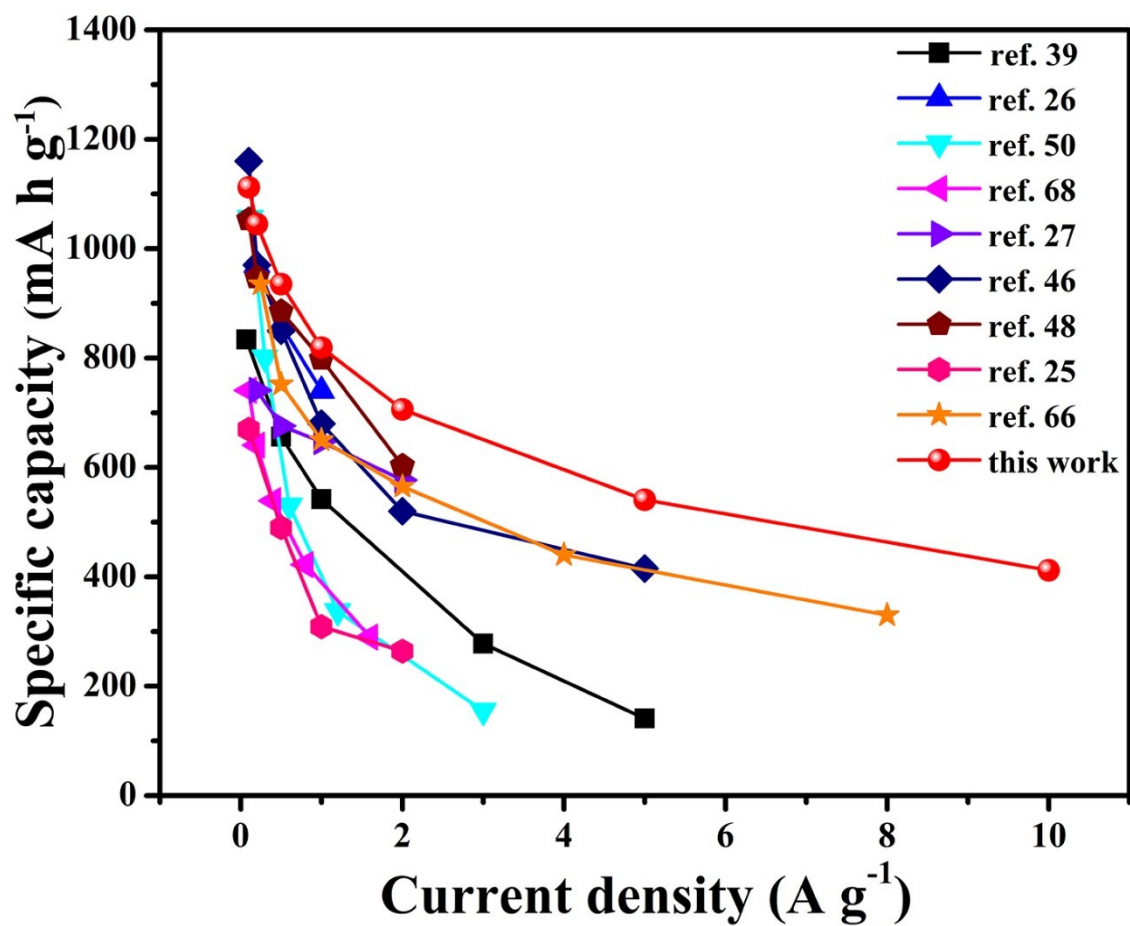


Fig. S10. Comparisons of the rate performance between the NiS₂/CNHs electrode in this work and the previously reported NiS_x-based anode materials.

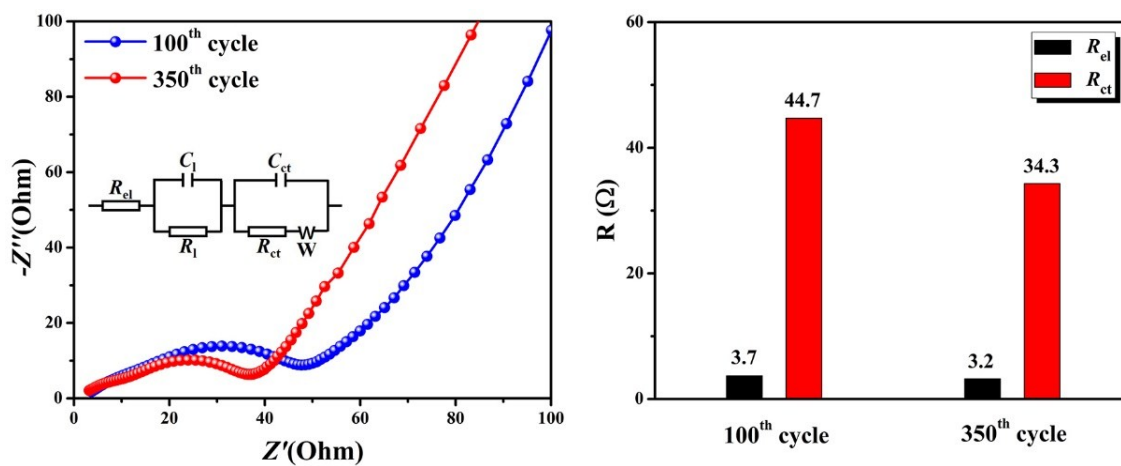


Fig. S11. (a) EIS of the NiS₂/CNHs electrode in LIBs at the 100th cycle and 350th cycle tested at a current density of 5 A g⁻¹, where the inset shows the equivalent circuit diagram. (b) Comparisons of R_{el} and R_{ct} values between the 100th cycle and 350th cycle, which are obtained according to the equivalent circuit diagram in (a).

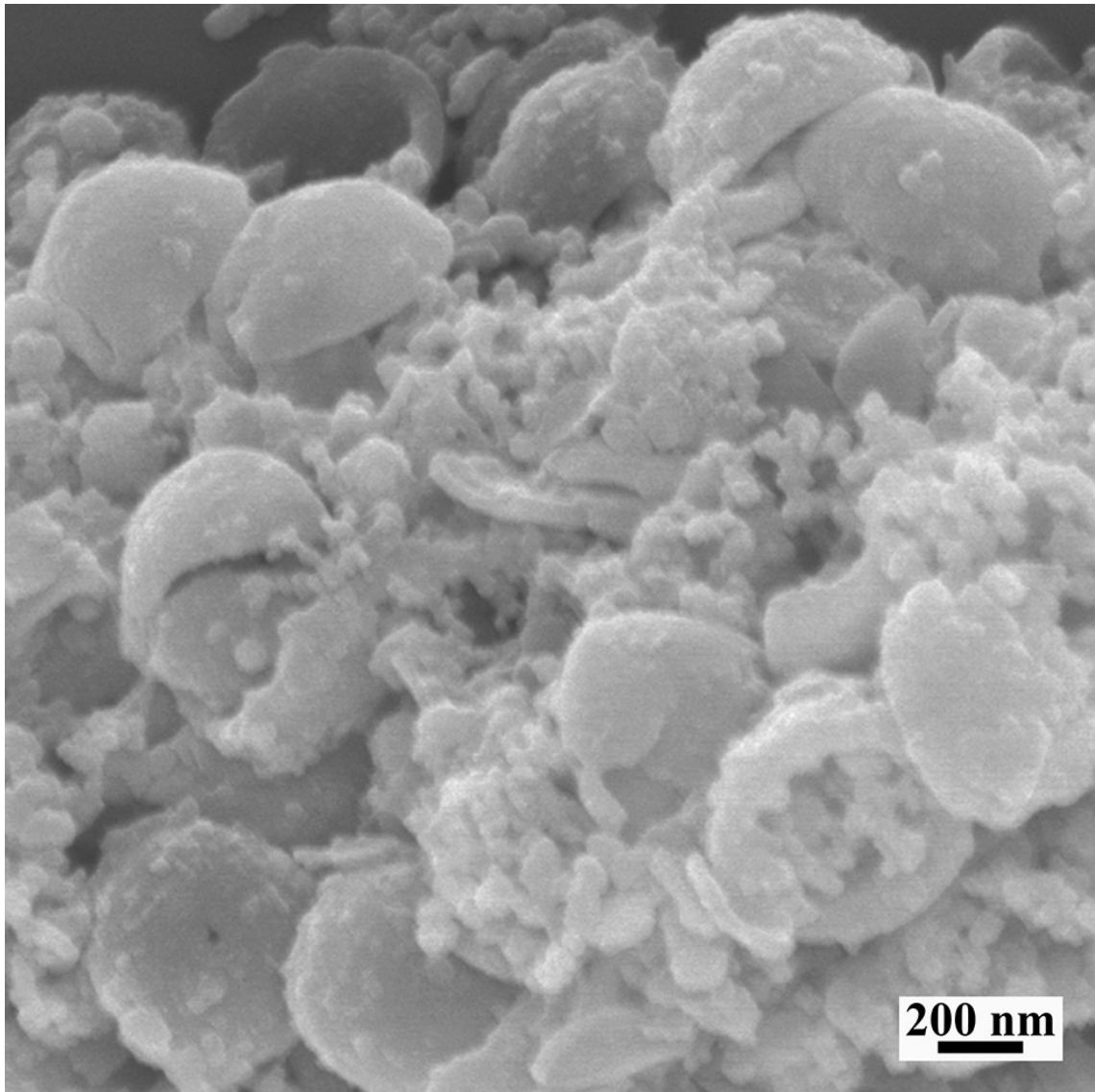


Fig. S12. FESEM image of the NiS₂/CNHs electrode after 2000 cycles.

Supplementary Table

Table S1. Comparisons of the rate and cycling performances of nickel sulfide anode materials in LIBs reported in open literature.

Material	Rate performance	Cycling performance	Ref.
NiS ₂ /CNHs	541 mA h g ⁻¹ (5 A g ⁻¹) 412 mA h g ⁻¹ (10 A g ⁻¹)	490 mA h g ⁻¹ (3000 cycles, 5 A g ⁻¹)	This work
NiO@β-NiS@Ni ₃ S ₂	160 mA h g ⁻¹ (3.2 A g ⁻¹)	498.5 mA h g ⁻¹ (100 cycles, 0.5 A g ⁻¹)	Ref. [68] of the text
NiS ₂ @rGO nanocomposites	603 mA h g ⁻¹ (2 A g ⁻¹)	1053 mA h g ⁻¹ (200 cycles, 0.1 A g ⁻¹)	Ref. [48] of the text
NiS ₂ @CoS ₂ @C @C nanocubes	415 mA h g ⁻¹ (5 A g ⁻¹)	600 mA h g ⁻¹ (100 cycles, 1 A g ⁻¹)	Ref. [46] of the text
NiS ₂ hollow spheres	264 mA h g ⁻¹ (2C)	580.6 mA h g ⁻¹ (400 cycles, 0.2C)	Ref. [25] of the text
NiS-GNS-CNT aerogels	330 mA h g ⁻¹ (8 A g ⁻¹)	732 mA h g ⁻¹ (350 cycles, 0.5 A g ⁻¹)	Ref. [66] of the text
NS/G-10	141 mA h g ⁻¹ (5 A g ⁻¹)	622 mA h g ⁻¹ (200 cycles, 0.07 A g ⁻¹)	Ref. [39] of the text
CNF@NiS-2	664.3 mA h g ⁻¹ (3 A g ⁻¹)	543.8 mA h g ⁻¹ (100 cycles, 3 A g ⁻¹)	Ref. [67] of the text
NiS ₂ /graphene	740 mA h g ⁻¹ (1 A g ⁻¹)	810 mA h g ⁻¹ (1000 cycles, 0.5 A g ⁻¹)	Ref. [26] of the text
ACT/NiS ₂ -graphene	645 mA h g ⁻¹ (1C)	1016 mA h g ⁻¹ (400 cycles, 0.1C)	Ref. [24] of the text
Ni ₃ S ₂ @N-G	252 mA h g ⁻¹ (16 A g ⁻¹)	809 mA h g ⁻¹ (150 cycles, 0.05 A g ⁻¹)	Ref. [49] of the text